Experimental Dermatology

WILEY

Experimental Dermatology

RESEARCH ARTICLE OPEN ACCESS

Memory T-Cell Phenotype in Cutaneous T-Cell Lymphoma Is Modified by Germline Gene Gametocyte Specific Factor 1

Amelia Martínez Villarreal[1,2] | Jennifer Gantchev[3] | Pingxing Xie[4] | Philippe Lefrançois[2,4,5] | Brandon Ramchatesingh[1,2] | Ivan V. Litvinov[1,2,4]

[1]Faculty of Medicine and Health Sciences, Research Institute of the McGill University Health Centre, McGill University, Montreal, Quebec, Canada | [2]Division of Experimental Medicine, Faculty of Medicine and Health Sciences, McGill University, Montreal, Quebec, Canada | [3]Department of Neurosurgery, Brigham and Women's Hospital, Harvard Medical School, Boston, Massachusetts, USA | [4]Division of Dermatology, Faculty of Medicine and Health Sciences, McGill University, Montreal, Quebec, Canada | [5]Lady Davis Institute for Medical Research, Jewish General Hospital, McGill University, Montreal, Quebec, Canada

Correspondence: Ivan V. Litvinov (ivan.litvinov@mcgill.ca)

Received: 6 October 2024 | **Revised:** 10 April 2025 | **Accepted:** 1 May 2025

Funding: This work was supported by the Cancer Research Society (CRS)—CIHR Partnership Grant #25343, Canadian Institutes for Health Research (CIHR) Project Scheme Grant #426655, and by the Fonds de la Recherche du Québec–Santé #296643 to Ivan V. Litvinov. Amelia Martínez Villarreal received support from the CONACYT (Mexico) and the Ministère de l'Éducation et de l'Enseignement supérieur (Québec). Jennifer Gantchev receives support from the CIHR Postdoctoral fellowship. Philippe Lefrançois receives support from the Fonds de la Recherche du Québec—Santé (#312768 and #324151). Brandon Ramchatesingh receives support from the FRQS Doctoral fellowship.

Keywords: cutaneous T-cell lymphoma (CTCL) | gametocyte specific factor 1 (GTSF1) | prognostic biomarker | retrotransposons | Th2

ABSTRACT

Cutaneous T-cell lymphoma (CTCL) is a heterogeneous group of lymphoproliferative disorders characterised by skin infiltration by malignant memory T cells. While most patients will present with an indolent disease, others will follow a highly aggressive clinical course. Currently, defining disease prognosis remains challenging. Ectopic expression of gametocyte-specific factor 1 (GTSF1) has emerged as a potential prognostic biomarker. However, its contribution to CTCL carcinogenesis remains unknown. Here, we report that GTSF1 contributes to carcinogenesis by partially modifying the memory/effector phenotype of the malignant T cells. GTSF1 knockdown in CTCL cells led to T-cell activation and production of IFNγ and TNFα. Advanced stages of the disease are associated with decreased production of these cytokines. Notably, we show that patients classified with high expression of GTSF1 are associated with a worse disease prognosis. Taken together, our findings indicate that GTSF1 expression in CTCL cells allows them to acquire memory T-cell phenotype. Malignant memory T cells have a decreased production of immune-responsive cytokines, leading to a diminished immune response and disease progression. GTSF1 is an important candidate as a prognostic biomarker. Furthermore, understanding the specific function of GTSF1 might help develop novel targeted treatment options for CTCL patients.

1 | Introduction

Cutaneous T-cell lymphoma (CTCL) is a rare and heterogeneous group of malignancies, characterised by the skin infiltration by malignant memory T cells [1, 2]. Life expectancy in the early stages is similar to a healthy control population; in contrast, life expectancy in advanced stages is less than ~2–3 years [3]. Approximately 25%–30% of patients with early disease progress to advanced stages [4]. Therefore, it is imperative to identify patients who have a higher risk of progression. Current prognostic factors are mainly based on clinical evaluation and certain pathological parameters (e.g., large cell transformation) [4, 5]. However, their usefulness remains limited [6]. Ectopic expression of gametocyte-specific factor 1 (GTSF1) has been

consistently reported to be associated with an aggressive disease course [7–13]. Therefore, GTSF1 has emerged as a potential prognostic biomarker.

High GTSF1 expression has been identified in patient samples with advanced stage disease (i.e., ≥ stage IIB) compared to patients with benign dermatoses and normal skin [7–10, 12–14]. GTSF1 is essential for spermatogenesis and suppression of transposons. In mouse germline cells, it participates in a small RNA-guided silencing system called the piRNA pathway. This pathway identifies active transposons and recruits the silencing machinery [15]. In that model, GTSF1 grasps and stabilises piRNAs during their maturation [16]. Considering that the reactivation of transposons has been associated with carcinogenesis [17], the expression of GTSF1 is highly relevant to CTCL carcinogenesis. However, its role remains to be elucidated.

CTCL is a highly heterogeneous entity both at the clinical and at the molecular levels [18, 19]. Clinical features in different variants include erythematous patches/plaques, violaceous tumours, loss of pigmentation, single/multiple lesions, poikiloderma, skin atrophy and a plethora of other symptoms [20]. The diverse clinical presentations highlight the heterogeneity of this malignancy. In addition, molecular variability between patients displaying the same variant, between different lesions of a single patient and even between different time points of a single lesion has been reported [10, 21, 22].

Progression has been associated with a shift of the predominant cytokines expressed in skin lesions [23]. In early stages, affected skin displays a Th1 immune-responsive cytokine profile [24]. This profile is defined by high expression of STAT4 and production of IFNγ and TNFα. In late stages, patients present a polarisation towards a Th2 immune phenotype, characterised by the expression of IL-4 and IL-5 [13, 25, 26]. The mechanisms behind this cytokine profile shift and progression remain to be elucidated.

Here, we aimed to understand the contribution of GTSF1 to CTCL carcinogenesis and its impact on the phenotype of the malignant T cells. We reasoned that a detailed understanding of GTSF1 can help us discern its potential as a prognostic biomarker. Using clinical data and in vitro cell line models, we studied its role in CTCL. We observed that GTSF1 expression is associated with a memory T-cell phenotype. In our in vitro work, GTSF1 knockdown leads to T-cell activation and increased expression of the immune-responsive cytokines, IFNγ and TNFα. This is mirrored in our clinical data evaluation, where high GTSF1 expression was associated with a worse clinical prognosis. We posit that high expression of GTSF1 in CTCL patients can be used as a progression biomarker of aggressive disease and unfavourable tumour microenvironment. Furthermore, GTSF1 contributes to the maintenance of a memory T cell phenotype, impacting the immune responsiveness of these patients.

2 | Methods

2.1 | Patients and Samples

All patients were enrolled in this study with written informed consent and in accordance with the Declaration of Helsinki. Samples were obtained after the approval from The Ottawa Hospital Research Institute (REB study #20150896-01H), Research Institute of the McGill University Health Centre and affiliated hospitals (REB study #A09-M81-10A) and Laval University (REB study # 2011HES-22808). The patient cohort has been previously described [9]. Samples were obtained by punch biopsy of the lesional skin and processed into formalin-fixed, paraffin-embedded (FFPE) tissue blocks.

2.2 | Cell Culture

All cell lines are human. Mac2A, MyLa 2000 (herein referred as MyLa), PB2B, HuT 78 and N/TERT-1 are male-derived cell lines, while SZ4 and Calu-6 are female-derived cell lines. Mac2A (RRID:CVCL_H637), MyLa (RRID:CVCL_8328), PB2B and SZ4 were obtained from Dr. K. Kaltoft and Dr. N. Ødum (University of Copenhagen, Copenhagen, Denmark). N/TERT-1 (RRID:CVCL_CW92) was obtained from Dr. J. Rheinwald (Harvard Medical School, Boston, USA). Calu-6 (ATCC Cat# HTB-56 RRID:CVCL_0236) and HuT78 (ATCC Cat# TIB-161 RRID:CVCL_0337) were purchased from the ATCC. All cell lines were cultured in their recommended media with the recommended percentage of Fetal Bovine Serum (FBS; Gibco Cat# 12484028) and 1% penicillin–streptomycin (p-s; Gibco Cat# 15140122). Cells were maintained at 37°C in a humidified incubator containing 5% CO_2.

2.3 | Immunohistochemistry

To evaluate the expression of GTSF1 in CTCL samples, we performed immunohistochemistry staining using the Bond III system (Leica) with GTSF1 antibody (Abnova Cat# PAB23356 RRID:AB_11125113) and HRP-conjugated compact polymer system and DAB (3, 3′-diaminobenzidine). Slides were counterstained with haematoxylin. Slides were scanned with Aperio AT Turbo system (Leica).

2.4 | Lentiviral shRNA-Mediated Knockdown

To perform shRNA-mediated knockdown of GTSF1, we transduced cell lines with a lentiviral vector. GIPZ Lentiviral shRNA vectors were purchased from Horizon Discovery: Clone V2LHS_24307 (Cat# VGH5518-200211965), clone V3LHS_304723 (Cat# VGH5518-200265235) and clone V3LHS_304726 (Cat# VGH5518-200299947). The GIPZ non-silencing vector (Cat# RHS4348) was used as a negative control. Transduction was performed with polybrene (Millipore Sigma Cat# TR-1003-G). Cells were selected with puromycin followed by GFP-sorting with a BD FACSAria Fusion (BD Biosciences). Clone V2LHS_24307 was selected to perform all experiments.

2.5 | RT-qPCR Analysis of Gene Expression

To evaluate RNA expression levels, we performed RT-qPCR. RNA was isolated with a RNeasy Mini Kit (Qiagen Cat# 74104) following the manufacturer's protocol. RNA was converted into cDNA with the iScript Advanced cDNA Kit for RT-qPCR (Bio-rad

Cat#1725038). Gene expression levels were evaluated with qPCR using SsoAdvanced Universal SYBR Green Supermix (Bio-rad Cat# 1725274) with the CFX Connect Real-Time PCR Detection System (Bio-rad). The housekeeping genes *GAPDH* or *ACTB* were used for standardisation following the Delta–Delta Ct Method.

2.6 | Dual-Luciferase Retrotransposition Assay

To evaluate the reactivation of retrotransposons, we performed an assay based on dual-luciferase measurement. Plasmids pYX014, pYX015 and pYX017 were obtained from Dr. Wenfeng An (South Dakota State University, USA) [27]. Cells were transiently transfected with Cell Line Nucleofector Kit V (Lonza Cat# VCA-1003) and Lonza Nucleofector Transfection 2b Device (Lonza RRID:SCR_022262). Luminescence was detected according to the manufacturer's protocol of Dual-Luciferase Reporter Assay System (Promega Cat # E1910) with an Infinite M200 PRO (Tecan RRID:SCR_019033) microplate reader. Each firefly luminescence value was divided by its corresponding *Renilla* value to correct for transfection efficiency and cell survival. Ratios corresponding to pYX015 were used as normalisation factors.

2.7 | Cell Proliferation Assay

Cell proliferation was measured using the Vi-CELL XR (Beckman Coulter RRID:SCR_019664) every 24 h until 144 h.

2.8 | Apoptosis Assay

To evaluate cell survival, we performed annexin V/PI staining. Cells were resuspended in annexin V binding buffer, stained with propidium iodide (PI; Invitrogen Cat# P1304MP) and 1 μL of annexin V, Alexa Fluor 647 conjugate (Invitrogen Cat# A23204). Cells were acquired in a BD FACSCanto II system (BD Biosciences RRID:SCR_018056) with BD FACSDiva Software (Version 8.0.2 BD Biosciences RRID:SCR_001456). Data analysis was performed using the FlowJo software (Version 10.9.0 BD Life Sciences RRID:SCR_008520).

2.9 | Immunofluorescence

To evaluate proliferation, we performed immunofluorescence staining for Ki67. The following antibodies were used: Ki67 primary antibody (Invitrogen Cat# PA5-16785 RRID:AB_11000602) and secondary Anti-rabbit Alexa Fluor 594 Conjugate (Cell Signaling Cat# 8889 RRID:AB_2716249). Cover slips were mounted on slides with Fluoroshield with DAPI (Millipore Sigma Cat# F6057). Visualisation and photos were acquired with a Lumascope LS720 microscope (Etaluma). Positive cells were quantified with QuPath (version 0.4.4 RRID:SCR_018257).

2.10 | Flow Cytometry Analysis of Cell Surface Markers

To evaluate changes in cell surface marker, we performed staining followed by flow cytometry analysis. Cells were stained with eBioscience Fixable Viability Dye eFluor 780 (Invitrogen Cat# 65-0865-14). The BD Horizon Brilliant Stain Buffer (BD Biosciences Cat# 563794) was used for staining with the fluorochrome-conjugated antibody BV421-CD25 (Biolegend Cat# 302630 RRID:AB_11126749). Cells were acquired in the BD FACSCanto II system (BD Biosciences) with BD FACSDiva Software (Version 8.0.2 BD Biosciences). Data analysis was performed using the FlowJo software (Version 10.9.0 BD Life Sciences).

2.11 | Cytokine Membranes

To evaluate cytokine dysregulation, we tested cell culture supernatant with a Human Th1/Th2/Th17 Antibody Array (Abcam Cat# ab169809), as per the manufacturer's protocol. Detection was performed in a ChemiDoc MP Imaging System (Bio-rad RRID:SCR_019037). Quantification was performed with the Image Lab Software (Version 6.1 Bio-rad RRID:SCR_014210).

2.12 | ELISA Assays

To quantify production of relevant cytokines, IFNγ (Invitrogen Cat# BMS228) and TNFα (Abcam Cat# ab181421), we performed ELISAs, as per the manufacturer's protocol. Absorbance values were measured with an Infinite M200 PRO (Tecan) microplate reader and corrected with the blank wells. The standard curve was plotted with the online Quest Graph Four Parameter Logistic (4PL) Curve Calculator (AAT Bioquest https://www.aatbio.com/tools/four-parameter-logistic-4pl-curve-regression-online-calculator).

2.13 | Extracellular Lactate Detection

To evaluate metabolic changes of memory/effector cells, we quantified lactate secretion using the Lactate-Glo Assay Kit (Promega Cat# J5021), as per the manufacturer's protocol. Luminescence was recorded with an Infinite M200 PRO (Tecan) microplate reader and normalised to growth media alone.

2.14 | Western Blotting

To evaluate protein expression, we performed western blotting with 4%–20% Mini-PROTEAN TGX Stain-Free Precast Gels (Bio-rad Cat# 4568093 and 4568094), followed by transfer to 0.22 μm PVDF membranes (Bio-rad Cat# 1704157 and 1704156). Overnight incubation at 4°C was carried out with the following primary antibodies: DDX4 (Abcam Cat# ab27591 RRID:AB_11139638), GAPDH (Thermo Fisher Scientific Cat# PA1-987 RRID:AB_2107311), GTSF1 (Abcam Cat# ab262937), LINE-1 Orf1p (Millipore Sigma Cat# MABC1152 RRID:AB_2941775), NFκB2 p100/p52 (Cell Signaling Cat# 4882 RRID:AB_10695537), PIWIL2 (Abcam Cat# ab181340), PIWIL4 (Abcam Cat# ab111714 RRID:AB_10887762), pSTAT3 Y705 (Cell Signaling Cat# 9145 RRID:AB_2491009), STAT3 (Cell Signaling Cat# 30835 RRID:AB_2798995), STAT4 (Cell

Signaling Cat# 2653, RRID:AB_2255156), STAT5 (Cell Signaling Cat# 94205 RRID:AB_2737403), pSTAT6 (Cell Signaling Cat# 9361 RRID:AB_331595), STAT6 (Cell Signaling Cat# 5397 RRID:AB_11220421) and TDRD9 (Abcam Cat# ab118427). Secondary antibody incubation for 1 h was performed with the appropriate HRP-conjugated secondary antibody: anti-mouse IgG (Cell Signaling Cat# 7076 RRID:AB_330924) or anti-rabbit IgG (Cell Signaling Cat# 7074 RRID:AB_2099233). For the chemiluminescence reaction, the Clarity Western ECL Substrate kit (Bio-rad Cat# 1705061) was used, and detection was performed in a ChemiDoc MP Imaging System (Bio-rad). Image processing was done with Image Lab Software (Version 6.1 Bio-rad).

2.15 | Bulk RNA-Sequencing

To evaluate the transcriptomic changes, we performed bulk RNA-Sequencing. RNA was isolated with an RNeasy Mini Kit (Qiagen Cat# 74104) following the manufacturer's protocol. Quality analysis, library preparation and sequencing were performed by Génome Québec.

2.16 | Analysis of RNA-Seq From Cell Lines

RNA-Seq analysis [28–32] was performed by the Rnomics platform at the Université de Sherbrooke. DESeq2 (Version 1.34 RRID:SCR_015687) was used to identify Differentially Expressed Genes (DEGs) between SCR control and shGTSF1 knockdown conditions. Functional enrichment analysis was performed with DEGs at Log_2 fold change ≥ 1 or Log_2 fold change ≤ -1 and p-adj < 0.05 using g:Profiler (Version e109_eg56_p17_1d3191d RRID:SCR_006809) [33–35]. The Venny 2.1 software was used to identify common DEGs. Gene lists used in heatmaps were accessed from KEGG Database [36].

2.17 | Analysis of Publicly Available Datasets

For analysis of The Cancer Genome Atlas (TCGA), RNA-Seq data from 33 cancers were downloaded from cBioPortal (RRID:SCR_014555) [37–39]. Mean Transcript Per Million (TPMs) were compared with Bayesian analysis using Markov Chain Monte Carlo with rjags (Version 4.3.0 RRID:SCR_017573) [40]. Multiple hypothesis testing adjustment was performed with the Bonferroni method.

For the CTCL dataset, RNA-Seq data (GEO accession number: GSE168508) [41] were obtained along with clinical data [42, 43]. For survival analysis, patients were ranked based on *GTSF1* mRNA level of expression. The upper tertile was classified as high and the two lower tertiles were classified as low, as previously described [44]. Differential expression was evaluated with the Mann–Whitney test and survival analysis was performed with the Log-rank (Mantel-Cox) test.

2.18 | Quantification and Statistical Analysis

Graphs and statistical analyses were performed using the software GraphPad Prism (Version 10.0.1 RRID:SCR_002798). Normality assumptions were tested with Shapiro–Wilk analysis and the F test. If normality assumptions were met, differences between means of three biological replicates were determined by a t test. In the case of multiple comparisons, the Mann–Whitney test was used with the Holm-Šídák correction method. Error bars represent standard deviation, and statistical significance was considered at $p < 0.05$. Figures were created using Inkscape (Version 1.2 RRID:SCR_014479).

3 | Results

To study the role of ectopic expression of GTSF1 in carcinogenesis, we evaluated gene expression data from TCGA. We compared the level of *GTSF1* mRNA expression between cancer and their normal adjacent tissue across 33 cancer types (Figure 1A). Our analysis demonstrated that *GTSF1* is significantly overexpressed in Breast Invasive Carcinoma (BRCA), Head and Neck Squamous Cell Carcinoma (HNSC), Kidney Renal Clear Cell Carcinoma (KIRC) and Kidney Renal Papillary Cell Carcinoma (KIRP). In addition, Acute Myeloid Leukaemia (LAML), Lymphoid Neoplasm Diffuse Large B-cell Lymphoma (DLBC) and Testicular Germ Cell Tumours (TGCT) showed a high level of expression. For this set of malignancies, no normal adjacent tissue data were available. This highlights that *GTSF1* is heterogeneously ectopically expressed across different cancer types. Considering its ectopic expression has been consistently reported in CTCL, we hypothesised that this indicates a particular and specific role in carcinogenesis of this lymphoma.

To evaluate the impact ectopic expression of GTSF1 has on CTCL prognosis/disease outcome, we conducted a survival analysis with a publicly available dataset (GEO accession number: GSE168508) [41]. We ranked patients based on the level of *GTSF1* mRNA expression and classified them in high versus low [44] expression groups (Figure 1B). Interestingly, the two patients with the most advanced stage (IVB) were classified in the high *GTSF1* expression group (Figure 1C). Furthermore, patients in the high *GTSF1* expression group had decreased overall survival and accelerated disease progression compared to patients in the low expression group (Figure 1D), particularly patients at disease stage IIB (Figure S1A). To evaluate GTSF1 expression at the protein level, we performed immunohistochemical staining of skin biopsies from CTCL patients (Figures 1E and S1B). GTSF1 expression was detected in a heterogeneous pattern. Some samples demonstrated nuclear GTSF1 expression in pleomorphic epidermotropic lymphocytes (Figure 1E, arrows).

Next, we sought to determine whether CTCL patient-derived cell lines expressed GTSF1. We performed RT-qPCR and western blot analysis with commonly used CTCL cell lines. These cell lines represent the most common variants of CTCL [45] (Figures 1F and S1C). All cell lines expressed GTSF1 mRNA and protein.

Previous publications reported that GTSF1 participates in the piRNA pathway, silencing retrotransposons during gametogenesis. Therefore, we hypothesised that GTSF1 expression in CTCL was associated with reactivation of this pathway and of

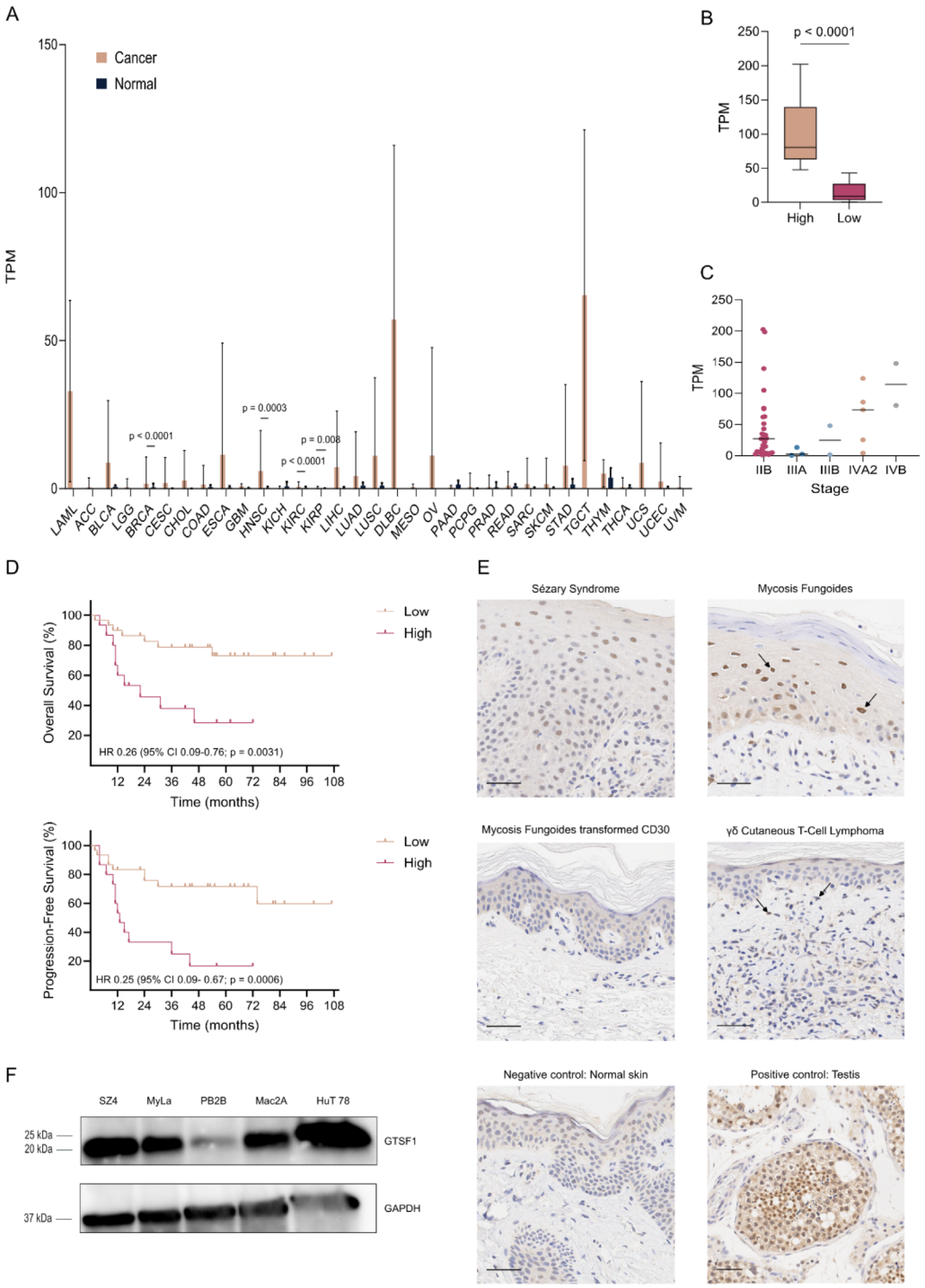

FIGURE 1 | Legend on next page.

retrotransposons. To test this, we analysed expression of other piRNA pathway elements (Figure 2A, top). Western blot of TDRD9, PIWIL4, DDX4 and PIWIL2 demonstrated a heterogeneous expression pattern. Of note, we did not observe expression of DDX4. The absence of DDX4 eliminates the possibility of piRNA pathway reactivation [46]. In addition, to evaluate the reactivation of retrotransposons we tested protein expression of the retrotransposon L1 (Figure 2A, bottom). The L1 protein ORF1p also demonstrated heterogeneous expression. Taken together, these results suggest that the piRNA pathway is not reactivated in selected CTCL cell lines at baseline.

Subsequently, we performed a lentiviral shRNA-mediated knockdown of GTSF1 in three cell lines. Considering that MF and SS represent > 50% of CTCL cases [47], selecting one cell line representative of each variant along with a cell line of pc-ALCL would represent the important clinical profiles in CTCL (Figures 2B and S2A,B). After GTSF1 knockdown, we evaluated whether it led to the reactivation or overexpression of retrotransposons. Unexpectedly, GTSF1 knockdown did not lead to increased expression of L1 mRNA (Figure S2C) nor ORF1p (Figure 2C). To evaluate changes in transposition events, we performed a dual-luciferase retrotransposition assay with two

FIGURE 1 | Heterogeneous GTSF1 expression in cancer and CTCL. (A) Relative *GTSF1* expression in Transcripts Per Million (TPM) for 33 cancer types (brown bars) and their normal counterparts (black bars) from The Cancer Genome Atlas (TCGA). Differential expression between cancer and normal adjacent tissue was evaluated with Markov Chain Monte Carlo and Bonferroni adjustment with $p < 0.05$. Data are presented as means ± SD. (B) Relative *GTSF1* expression in TPM in CTCL patients from GSE168508. Differential expression between high (brown bars) and low (pink bars) *GTSF1* was evaluated with Mann–Whitney test with $p < 0.05$, whiskeys represent minimum and maximum and lines in the middle of boxes represent the median. (C) Number of patients on each disease stage classified in high or low *GTSF1* expression from GSE168508. (D) Survival (Kaplan–Meier) plots of CTCL patients' disease outcomes: Overall Survival (top) and Progression-Free Survival (bottom). Differential survival between high (brown bars) and low (pink bars) *GTSF1* expression groups was identified with Log-rank (Mantel-Cox) test with $p < 0.05$. (E) Representative immunohistochemistry of GTSF1 in skin biopsies from CTCL patients. Each panel represents a different patient. Arrows indicate nuclear expression of GTSF1 in pleomorphic epidermotropic lymphocytes. Negative control (normal skin) is presented bottom left and positive control (normal human testis) is presented bottom right. Scale bars represent 50 μm. (F) Western blot analysis of GTSF1 in CTCL cell lines. GAPDH was used as a loading control. ACC, adrenocortical carcinoma; BLCA, bladder urothelial carcinoma; BRCA, breast invasive carcinoma; CESC, cervical squamous cell carcinoma and endocervical adenocarcinoma; CHOL, cholangiocarcinoma; COAD, colon adenocarcinoma; DLBC, lymphoid neoplasm diffuse large B-cell lymphoma; ESCA, oesophageal carcinoma; GBM, glioblastoma multiforme; HNSC, head and neck squamous cell carcinoma; KICH, kidney chromophobe; KIRC, kidney renal clear cell carcinoma; KIRP, kidney renal papillary cell carcinoma; LAML, acute myeloid leukaemia; LGG, brain lower grade glioma; LIHC, liver hepatocellular carcinoma; LUAD, lung adenocarcinoma; LUSC, lung squamous cell carcinoma; MESO, mesothelioma; OV, ovarian serous cystadenocarcinoma; PAAD, pancreatic adenocarcinoma; PCPG, pheochromocytoma and paraganglioma; PRAD, prostate adenocarcinoma; READ, rectum adenocarcinoma; SARC, sarcoma; SKCM, skin cutaneous melanoma; STAD, stomach adenocarcinoma; TGCT, testicular germ cell tumours; THCA, thyroid carcinoma; THYM, thymoma; UCEC, uterine corpus endometrial carcinoma; UCS, uterine carcinosarcoma; UVM, uveal melanoma.

different reporter plasmids, pYX014 and pYX017 [27]. GTSF1 knockdown did not lead to increased luminescence, highlighting that GTSF1 knockdown does not reactivate retrotransposon expression (Figure 1D). Taken together, these data indicate that GTSF1 expression in CTCL is not related to retrotransposon control.

Given the evidence of the role developmental program genes play in carcinogenesis, we evaluated the involvement of GTSF1 in CTCL cells' survival and proliferation. We hypothesised that the ectopic expression of GTSF1 suggests a dependency on this gene. To test this, we performed a cell proliferation assay from 24 h up to 144 h (Figure S3A). GTSF1 knockdown did not affect proliferation nor survival. Due to the limitations associated with this assay, we evaluated apoptosis and proliferation using assays with higher sensitivity.

To evaluate whether GTSF1 knockdown led to increased apoptosis, we performed annexin V/PI staining. We observed no increase in any apoptotic stage (Figure S3B). Then, to evaluate proliferation, we performed immunofluorescence staining for the proliferation marker Ki67. Quantification of $Ki67^+$ cells confirmed GTSF1 knockdown did not impact proliferation (Figure S3C). Together, these data suggest GTSF1 is not essential nor provides a selective growth advantage for the survival and proliferation of CTCL cells.

Considering these findings, we hypothesised the role of GTSF1 to be related to other hallmarks of cancer. To test this, we performed bulk RNA-Seq and identified DEGs between SCR and shGTSF1 cells (Figure S4). Surprisingly, volcano plots demonstrated markedly different profiles for each cell line (Figure 3A). To assess a common role of GTSF1 across the three cell lines, we created a Venn diagram from the DEGs of the three cell lines and considered the intersection of all three cell lines to increase robustness (Figure 3B). This rendered four genes: GTSF1, validating the knockdown; ANO1, a calcium-activated channel; ITGB7, a member of the integrin superfamily; and Lnc-CCAR2-2, a lnRNA without any previously described role. Importantly, except for GTSF1, none of these genes presented the same direction of dysregulation. Together, these findings suggest that GTSF1 knockdown leads to a different transcriptomic profile for each CTCL variant: This is aligned with the fact that each cell line represents a clinically different entity [45, 48].

To better understand these different profiles, we evaluated the most common dysregulated pathways in CTCL: NF-κB, JAK–STAT and TCR signalling pathways [49] (Figure 3C). Consistent with earlier findings, each cell line presented a different expression profile for each pathway. Interestingly, Mac2A presented upregulation, MyLa presented both upregulation and downregulation, and SZ4 presented downregulation of genes in these pathways. To further evaluate these different profiles, we performed western blot of selected proteins of the NF-κB and JAK–STAT pathways (Figure 3D). This confirmed varying expression patterns for each cell line, with a trend of upregulation in Mac2A and downregulation in SZ4. Interestingly, Mac2A showed three NFKB2 bands: the precursor and active forms and a band of approximately 80 kDa. In CTCL, NFKB2 commonly displays C-terminal deletions rendering the NF-κB pathway constitutively active [50]. In addition, pSTAT3 and STAT3 showed increased expression after GTSF1 knockdown, suggesting activation of this signalling pathway. Changes in STAT4, STAT5 and STAT6 confirmed downregulation in SZ4. Taken together, these results suggest that the role of GTSF1 is CTCL variant dependent.

In CTCL, disease progression is associated with a Th2 phenotype/decreased immune response [51], which contrasts with the immune activation we observed for Mac2A. Given this clinical relevance, we sought to better understand these changes. Pathway enrichment analysis for Mac2A GTSF1 knockdown led to immune activation (Figures 4A and S5A). Top hit pathways included: defence response to virus, myeloid leukocyte activation and acute inflammatory response. Memory and effector

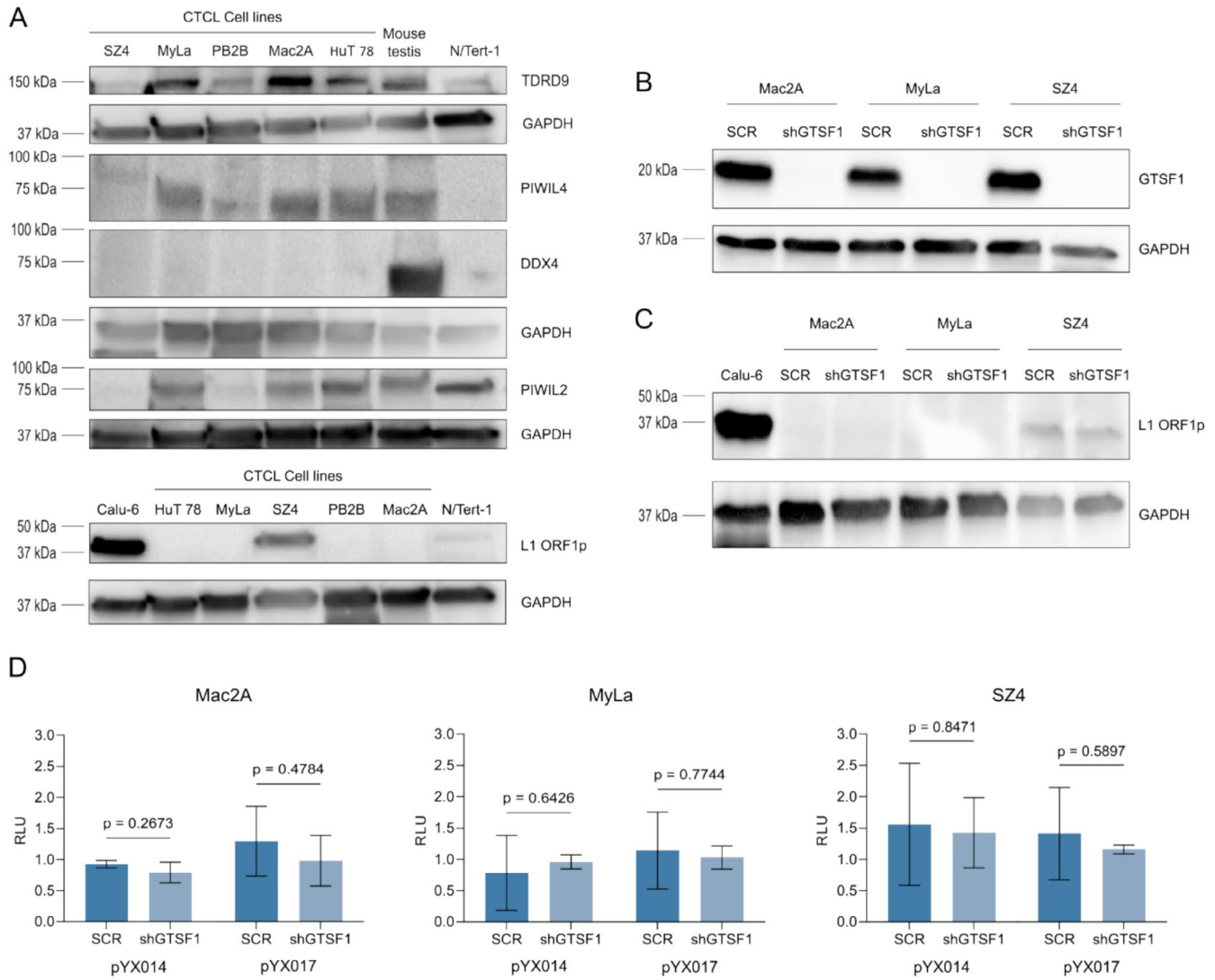

FIGURE 2 | In CTCL, GTSF1 does not regulate retrotransposons. (A) Western blot analysis of piRNA pathway elements TDRD9, PIWIL4, DDX4 and PIWIL2 (top) and of retrotransposon L1 ORF1p (bottom) in CTCL cell lines. Protein from mouse testis is used as a positive control (top), protein from cell line Calu-6 is used as a positive control (bottom) and protein from cell line N/Tert-1 (top and bottom) is used as a non-malignant control. GAPDH was used as a loading control and is presented for each membrane probed. (B) Western blot analysis of GTSF1 after lentiviral shRNA-mediated knockdown in the three CTCL cell lines Mac2A, MyLa and SZ4. GAPDH was used as a loading control. (C) Western blot analysis of L1 ORF1p after GTSF1 knockdown in CTCL cell lines. Protein from cell line Calu-6 is used as a positive control. GAPDH was used as a loading control. (D) Luciferase activity from retrotransposition assay in Relative Luminescence Units (RLU). Each assay was performed with two reporter plasmids, pYX014 and pYX017, for each cell line. Firefly luminescence was corrected with the corresponding *Renilla* luminescence value and the retrotransposition incompetent plasmid pYX015 is used to normalise luminescence values. Differences between SCR (dark blue bars) and shGTSF1 (light blue bars) were evaluated with unpaired two-tailed *t* test. Data are presented as means of three replicates ± SD.

T cells behave in a spectrum, with each phenotype at one extreme; movement towards an effector phenotype is caused by activation [52, 53]. Therefore, we evaluated the expression of genes associated with each extreme of the spectrum (Figure 4B). Interestingly, we identified increased expression of genes on both extremes. Knockdown led to increased expression of *IFNG* and *CXCR3*, both associated with effector phenotype and increased expression of *EOMES*, associated with T cell memory phenotype. Together, these findings suggest that GTSF1 knockdown led to a dysregulation in the memory/effector phenotype spectrum.

We then sought to better understand this dysregulation in the memory/effector phenotype. We evaluated activation by quantifying the percentage of $CD25^+$ cells as an indicator of activation (Figure 4C). The percentage of $CD25^+$ T cells remained unchanged after GTSF1 knockdown. Given that T-cell activation leads to cytokine production, we evaluated changes in cytokine production with a cytokine membrane. We identified multiple changes in cytokine production; however, none showed statistical significance. Interestingly, GTSF1 knockdown led to an increased production of the Th1-associated cytokines IFNγ and TNFα. In contrast, IL-2 showed no change (Figures 4D and S5B). Due to the importance of IFNγ and TNFα in the decline of the immune response in CTCL patients [51], we decided to validate these findings. ELISA assays demonstrated that GTSF1 knockdown led to significantly increased production of IFNγ and increased production of

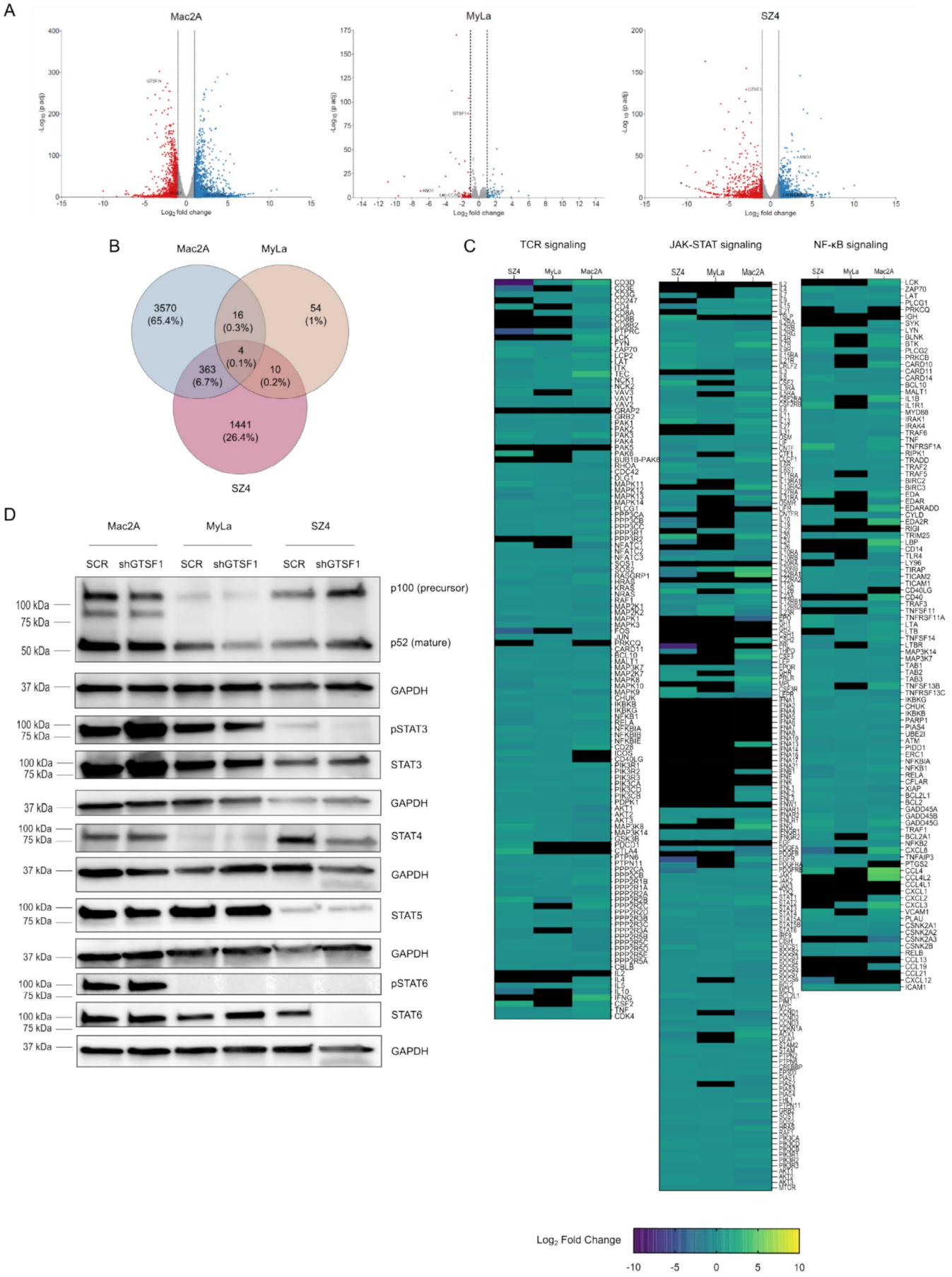

FIGURE 3 | Legend on next page.

FIGURE 3 | GTSF1 has a different role in each CTCL variant. (A) Volcano plots showing Log_2 fold change and $-Log_{10}$ (*p*-adj) after GTSF1 knockdown in CTCL cell lines. Each dot represents one gene. Upregulated genes (Log_2 fold change ≥ 1) are presented in blue, downregulated genes (Log_2 fold change ≤ −1) in red and genes with no significant change in grey. GTSF1, ANO1, ITGB7 and Lnc-CCAR2-2 are highlighted. (B) Venn diagram of common DEGs (Log_2 fold change ≥ 1 or (Log_2 fold change ≤ −1 and p-adj < 0.05) after GTSF1 knockdown in CTCL cell lines. Percentages in parenthesis are calculated from the total queried genes. (C) Heatmaps showing Log_2 fold change of gene expression between SCR and shGTSF1 for CTCL cell lines in the following pathways: TCR signalling (left), JAK–STAT signalling (middle), and NF-κB signalling (right). Each column represents a cell line and each row a gene. Gene lists were retrieved from the KEGG database. The Log_2 fold change expression scale is presented at the bottom. A black rectangle in the heatmap cell means no expression was detected. (D) Western blot analysis of NFKB2, pSTAT3, STAT3, STAT4, STAT5, pSTAT6 and STAT6 after GTSF1 knockdown in CTCL cell lines. GAPDH was used as a loading control and is presented for each membrane probed.

TNFα (Figure 4E). Next, we evaluated metabolic changes associated with the memory/effector T-cell phenotype. Effector cells rely on glycolysis and production of lactate, while memory cells rely on oxidative phosphorylation [54, 55]. Therefore, we measured extracellular production of lactate (Figure 4F). GTSF1 knockdown did not lead to changes in lactate secretion. This suggests that cells with low GTSF1 expression do not rely on glycolysis and/or production of lactate. Taken together, these data suggest GTSF1 plays a partial role in modifying the memory/effector phenotype in CTCL cells, particularly in the production of cytokines associated with immune activation.

4 | Discussion

Ectopic expression of germline genes is a well-established finding in cancer [56]. Despite this, the specific functions many of these genes perform in carcinogenesis remain poorly understood [57]. In CTCL, ectopic expression of GTSF1 and its association with worse clinical prognosis has been consistently reported [8–13, 24]. Interestingly, ectopic expression of GTSF1 has also been reported in Acute Myeloid Leukaemia [58, 59] and liver cancer [60]. However, the role of GTSF1 in carcinogenesis remains unknown. Here, we aimed to understand its contribution to CTCL carcinogenesis and its impact on malignant T-cell phenotype.

Previous publications associating GTSF1 expression with a worse prognosis did so by including it as a member of a gene cluster [8, 9, 24]. We demonstrate that for patients in disease stage IIB, GTSF1 expression on its own is associated with accelerated cancer progression and decreased survival—worse overall prognosis. In agreement with previous publications [8, 9, 12, 13, 24], our analysis shows that patients with the most advanced stage of the disease display high GTSF1 expression. Our immunohistochemistry analysis demonstrates a heterogeneous expression pattern in tissues. High genetic/molecular heterogeneity is a well-established characteristic of CTCL [19, 21, 61]. Therefore, we reason that GTSF1 is an interesting candidate as a progression biomarker for CTCL.

In mouse germline cells, GTSF1 participates in the piRNA pathway, silencing active retrotransposons [16, 62]. Although retrotransposon reactivation and function have been previously reported in CTCL [63], our results indicate that the piRNA pathway is not reactivated. Our results also indicate that GTSF1 knockdown does not lead to an increased rate of retrotransposition events from its baseline. In agreement, previous publications demonstrated that the ectopic expression of other piRNA elements in cancer did not lead to pathway reactivation [46, 64].

Our investigation suggests that in CTCL, GTSF1 partially controls the memory/effector phenotype of the malignant T cells. CTCL arises from skin resident memory T cells [61, 65], which means these cells are inactive. When memory T cells re-encounter their cognate antigen, they acquire effector phenotype characteristics [54, 66]. GTSF1 knockdown led to T-cell activation and production of IFNγ and TNFα cytokines. This suggests that GTSF1 knockdown leads to an acquisition of effector phenotype. Although not all effector phenotype markers we evaluated demonstrated a change, this is in line with memory/effector T cells behaving on a spectrum [53, 55, 67]. Interestingly, a recent publication proposed a molecular classification for CTCL based on the malignant T cells and their microenvironment expression profile [11]. The central memory T-cell profile is associated with GTSF1 expression. Therefore, we speculate that GTSF1 partially modifies the memory/effector phenotype, tilting the balance towards the memory T-cell phenotype.

Disease progression is associated with a shift in the type of cytokines produced in the skin. In early stage disease, skin samples show production of the Th1 immune-responsive cytokines IFNγ and TNFα, while in late stages the cytokines produced are the Th2/immune-repressive IL-4 and IL-5 [25, 26]. Our data show the negative role GTSF1 has in controlling the production of cytokines associated with early stage disease. Furthermore, this is mirrored in our patient data analysis, in which patients with high GTSF1 expression demonstrate poor survival. We speculate that GTSF1 modulates early stage cytokines, impacting disease progression.

Here, we present an initial mechanistic study to understand the role of GTSF1 in CTCL. With in vitro approaches, we demonstrate the role of GTSF1 in modifying the memory-effector phenotype of malignant cells. Studies with in vivo models, other variants of CTCL, and additional patient data will help address this limitation. Specifically, we show that only the cell line Mac2A, representative of pc-ALCL, responded to GTSF1 silencing. Whether this reflects the mutational status of Mac2A, the variant of CTCL it represents, or even the expression of CD30 is of utmost importance to answer. Furthermore, recent publications have reported that ALCL presents a Th17 profile [68]. In addition to the production of IL-17, the Th17 profile is also associated with high STAT3 activity and low expression of GATA3 [68]. Our data show that GTSF1 knockdown in Mac2A led to higher transcript expression of *IL17D* and *IL17F* (data not shown) and activation of STAT3; however, GATA3 did not show

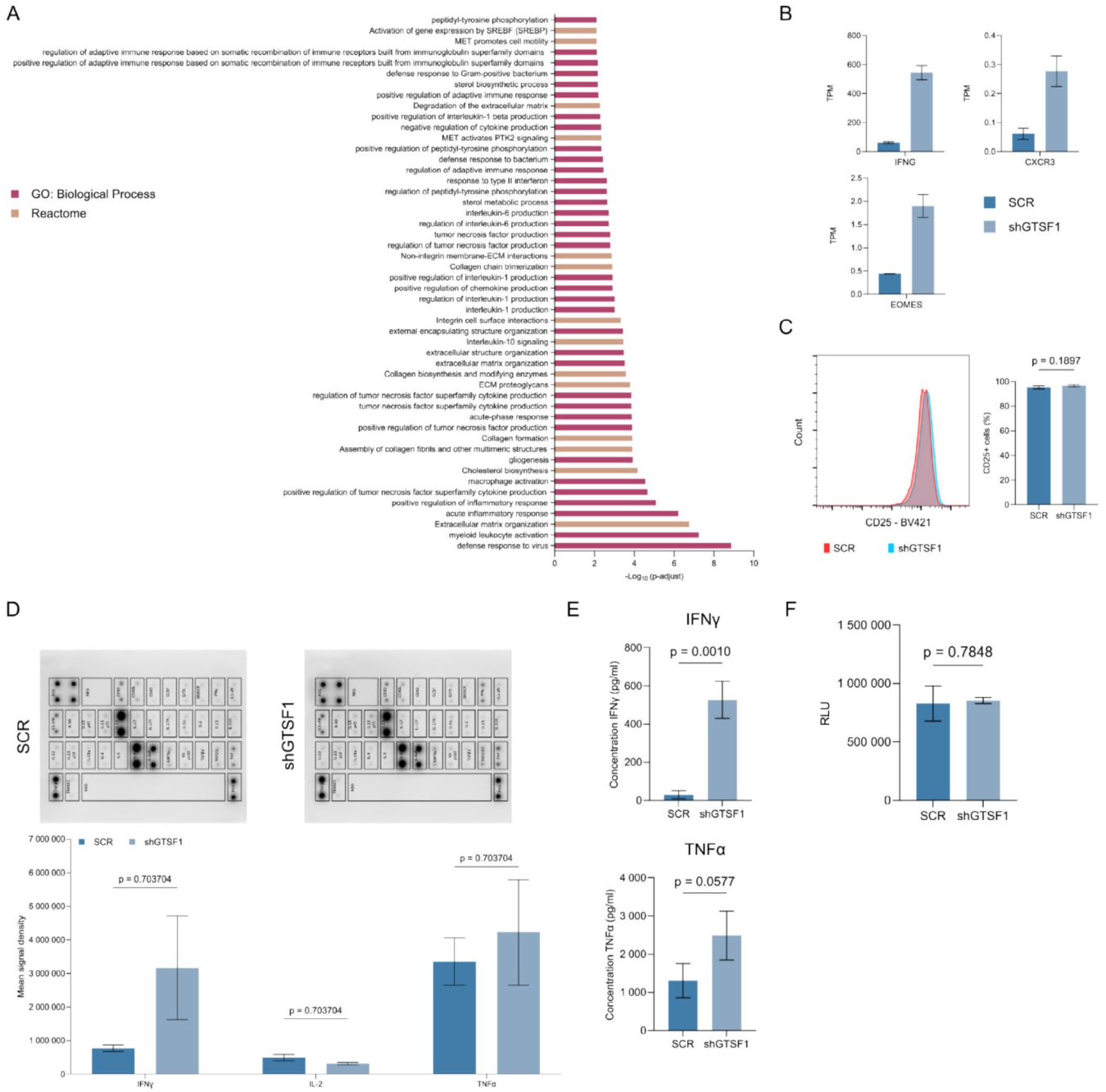

FIGURE 4 | GTSF1 modifies the memory/effector phenotype. (A) Pathway enrichment analysis showing $-\text{Log}_{10}$ (p-adj) of the top 50 significantly dysregulated pathways after GTSF1 knockdown in Mac2A. Pathways from Gene Ontology (GO): Biological Processes are shown in pink and pathways from Reactome are shown in brown. (B) Relative expression in Transcripts Per Million (TPM) of selected DEGs in SCR (dark blue) and shGTSF1 (light blue) in Mac2A. Data are presented as means of three replicates ± SD. (C) Flow cytometry analysis of CD25 cell surface marker expression. Representative histogram (left) from SCR (red) and shGTSF1 (blue). Percentage of $CD25^+$ (right) cells. Differences between SCR (dark blue) and shGTSF1 (light blue) were evaluated with unpaired two-tailed t test. Data are presented as means of three replicates ± SD. (D) Cytokine production analysis after GTSF1 knockdown in Mac2A. Representative membranes (top) from SCR and shGTSF1 are presented. Mean signal density (bottom) of selected cytokines. Differences between SCR (dark blue bars) and shGTSF1 (light blue bars) were evaluated with Mann–Whitney test and Holm-Šídák correction method. Data are presented as means of two replicates ± SD. (E) ELISA assays for quantification of IFNγ (top) and TNFα (bottom) production after GTSF1 knockdown in Mac2A. Differences between SCR (dark blue bars) and shGTSF1 (light blue bars) were evaluated with unpaired two-tailed t test. Data are presented as means of three replicates ± SD. (F) Luciferase activity from lactate secretion assay in Relative Luminescence Units (RLU). Differences between SCR (dark blue bars) and shGTSF1 (light blue bars) were evaluated with unpaired two-tailed t test. Data are presented as means of three replicates ± SD.

differential expression. Therefore, future research should consider evaluating the Th17 profile in detail.

Together, our data places GTSF1 as a candidate for a putative disease progression biomarker. Given the heterogeneity that characterises CTCL, its robustness as a biomarker needs to be validated by other groups. Additionally, as a germline gene, GTSF1 has potentially immunogenicity and privileged expression, making it a strong candidate for the development of immunotherapies [57]. We speculate that targeting GTSF1-expressing cells will allow us to tilt the balance towards the effector phenotype. Favouring an effector phenotype will then lead to an immune-responsive profile in CTCL patients. Thus, our data suggest that the ectopic expression of germline genes in cancer may allow the malignant cells to recapture the function of these genes in a novel way for their benefit. Understanding the role these genes play in carcinogenesis can help us discern the best candidates for novel treatments.

Author Contributions

A.M.V. designed research, performed experiments, analysed and interpreted data, performed statistical analysis and wrote the manuscript. J.G. designed research and performed experiments. P.X. and P.L. analysed data and performed statistical analysis. B.R. edited the manuscript. I.V.L. designed research, analysed and interpreted data, provided resources and supervised the study. All authors have read and agreed to the published version of the manuscript.

Acknowledgements

The authors thank Génome Québec for sequencing services, the RNomics Platform at the Université de Sherbrooke for bioinformatic services, the pathology department of The Ottawa Hospital Research Institute for immunohistochemistry services, the Histopathology platform of the RI-MUHC for slide scanning services and the Immunophenotyping platform of the RI-MUHC for sorting and flow cytometry services. The authors thank Dr. Danny Bergeron from the RNomics Platform for the analysis of RNA-Seq data. One graph shown here is based upon data generated by the TCGA Research Network: https://www.cancer.gov/tcga.

Ethics Statement

All patients were enrolled in this study with written informed consent and in accordance with the Declaration of Helsinki. Samples were obtained after approval from The Ottawa Hospital Research Institute (REB study #20150896-01H), Research Institute of the McGill University Health Centre and affiliated hospitals (REB study #A09-M81-10A) and Laval University (REB study # 2011HES-22808). The patient cohort has been previously described [9]. Samples were obtained by punch biopsy of the lesional skin and processed into formalin-fixed, paraffin-embedded (FFPE) tissue blocks.

Conflicts of Interest

The authors declare no conflicts of interest.

Data Availability Statement

RNA-Seq data have been deposited in Gene Expression Omnibus database under accession number GSE270818. Original data sets generated and/or analysed here and not available in GEO are available on request from first author Amelia Martinez Villarreal (amelia.martinezvillarreal@mail.mcgill.ca).

References

1. P. Lefrancois, P. Xie, L. Wang, et al., "Gene Expression Profiling and Immune Cell-Type Deconvolution Highlight Robust Disease Progression and Survival Markers in Multiple Cohorts of CTCL Patients," *Oncoimmunology* 7, no. 8 (2018): e1467856.

2. I. V. Litvinov, A. Shtreis, K. Kobayashi, et al., "Investigating Potential Exogenous Tumor Initiating and Promoting Factors for Cutaneous T-Cell Lymphomas (CTCL), a Rare Skin Malignancy," *Oncoimmunology* 5, no. 7 (2016): e1175799.

3. F. M. Ghazawi, N. Alghazawi, M. Le, et al., "Environmental and Other Extrinsic Risk Factors Contributing to the Pathogenesis of Cutaneous T Cell Lymphoma (CTCL)," *Frontiers in Oncology* 9 (2019): 300.

4. P. L. Zinzani, A. J. Ferreri, and L. Cerroni, "Mycosis Fungoides," *Critical Reviews in Oncology/Hematology* 65, no. 2 (2008): 172–182.

5. C. Su, R. Tang, H. X. Bai, et al., "Disease Site as a Prognostic Factor for Mycosis Fungoides: An Analysis of 2428 Cases From the US National Cancer Database," *British Journal of Haematology* 185, no. 3 (2019): 592–595.

6. G. M. Amorim, J. P. N. Corbellini, D. C. Quintella, T. Cuzzi, and E. S. M. Ramos, "Evaluation of the Cutaneous Lymphoma International Prognostic Index in Patients With Early Stage Mycosis Fungoides," *Anais Brasileiros de Dermatologia* 93, no. 5 (2018): 680–685.

7. I. V. Litvinov, B. Cordeiro, Y. Huang, et al., "Ectopic Expression of Cancer-Testis Antigens in Cutaneous T-Cell Lymphoma Patients," *Clinical Cancer Research* 20, no. 14 (2014): 3799–3808.

8. I. V. Litvinov, E. Netchiporouk, B. Cordeiro, et al., "The Use of Transcriptional Profiling to Improve Personalized Diagnosis and Management of Cutaneous T-Cell Lymphoma (CTCL)," *Clinical Cancer Research* 21, no. 12 (2015): 2820–2829.

9. I. V. Litvinov, M. T. Tetzlaff, P. Thibault, et al., "Gene Expression Analysis in Cutaneous T-Cell Lymphomas (CTCL) Highlights Disease Heterogeneity and Potential Diagnostic and Prognostic Indicators," *Oncoimmunology* 6, no. 5 (2017): e1306618.

10. X. Liu, S. Jin, S. Hu, et al., "Single-Cell Transcriptomics Links Malignant T Cells to the Tumor Immune Landscape in Cutaneous T Cell Lymphoma," *Nature Communications* 13, no. 1 (2022): 1158.

11. K. Rindler, C. Jonak, N. Alkon, et al., "Single-Cell RNA Sequencing Reveals Markers of Disease Progression in Primary Cutaneous T-Cell Lymphoma," *Molecular Cancer* 20, no. 1 (2021): 124.

12. M. S. van Kester, M. K. Borg, W. H. Zoutman, et al., "A Meta-Analysis of Gene Expression Data Identifies a Molecular Signature Characteristic for Tumor-Stage Mycosis Fungoides," *Journal of Investigative Dermatology* 132, no. 8 (2012): 2050–2059.

13. M. Z. X. Xiao, D. Hennessey, A. Iyer, et al., "Transcriptomic Changes During Stage Progression of Mycosis Fungoides," *British Journal of Dermatology* 186, no. 3 (2022): 520–531, https://doi.org/10.1111/bjd.20760.

14. K. Rindler, W. M. Bauer, C. Jonak, et al., "Single-Cell RNA Sequencing Reveals Tissue Compartment-Specific Plasticity of Mycosis Fungoides Tumor Cells," *Frontiers in Immunology* 12 (2021): 666935.

15. C. Ernst, D. T. Odom, and C. Kutter, "The Emergence of piRNAs Against Transposon Invasion to Preserve Mammalian Genome Integrity," *Nature Communications* 8, no. 1 (2017): 1411.

16. T. Yoshimura, T. Watanabe, S. Kuramochi-Miyagawa, et al., "Mouse GTSF1 Is an Essential Factor for Secondary piRNA Biogenesis," *EMBO Reports* 19, no. 4 (2018): e42054.

17. K. H. Burns, "Transposable Elements in Cancer," *Nature Reviews. Cancer* 17, no. 7 (2017): 415–424.

18. J. Choi, G. Goh, T. Walradt, et al., "Genomic Landscape of Cutaneous T Cell Lymphoma," *Nature Genetics* 47, no. 9 (2015): 1011–1019.

19. A. Iyer, D. Hennessey, S. O'Keefe, et al., "Branched Evolution and Genomic Intratumor Heterogeneity in the Pathogenesis of Cutaneous T-Cell Lymphoma," *Blood Advances* 4, no. 11 (2020): 2489–2500.

20. A. C. Hristov, T. Tejasvi, and A. W. R, "Cutaneous T-Cell Lymphomas: 2021 Update on Diagnosis, Risk-Stratification, and Management," *American Journal of Hematology* 96, no. 10 (2021): 1313–1328.

21. T. B. Buus, A. Willerslev-Olsen, S. Fredholm, et al., "Single-Cell Heterogeneity in Sezary Syndrome," *Blood Advances* 2, no. 16 (2018): 2115–2126.

22. A. Iyer, D. Hennessey, S. O'Keefe, et al., "Independent Evolution of Cutaneous Lymphoma Subclones in Different Microenvironments of the Skin," *Scientific Reports* 10, no. 1 (2020): 15483.

23. G. Dobos, I. Lazaridou, and A. de Masson, "Mycosis Fungoides and Sezary Syndrome: Microenvironment and Cancer Progression," *Cancers (Basel)* 15, no. 3 (2023): 746.

24. I. V. Litvinov, B. Cordeiro, S. Fredholm, et al., "Analysis of STAT4 Expression in Cutaneous T-Cell Lymphoma (CTCL) Patients and Patient-Derived Cell Lines," *Cell Cycle* 13, no. 18 (2014): 2975–2982.

25. E. Guenova, R. Watanabe, J. E. Teague, et al., "TH2 Cytokines From Malignant Cells Suppress TH1 Responses and Enforce a Global TH2 Bias in Leukemic Cutaneous T-Cell Lymphoma," *Clinical Cancer Research* 19, no. 14 (2013): 3755–3763.

26. J. Ren, R. Qu, N. T. Rahman, et al., "Integrated Transcriptome and Trajectory Analysis of Cutaneous T-Cell Lymphoma Identifies Putative Precancer Populations," *Blood Advances* 7, no. 3 (2023): 445–457.

27. Y. Xie, J. M. Rosser, T. L. Thompson, J. D. Boeke, and W. An, "Characterization of L1 Retrotransposition With High-Throughput Dual-Luciferase Assays," *Nucleic Acids Research* 39, no. 3 (2011): e16.

28. A. M. Bolger, M. Lohse, and B. Usadel, "Trimmomatic: A Flexible Trimmer for Illumina Sequence Data," *Bioinformatics* 30, no. 15 (2014): 2114–2120.

29. N. L. Bray, H. Pimentel, P. Melsted, and L. Pachter, "Near-Optimal Probabilistic RNA-Seq Quantification," *Nature Biotechnology* 34, no. 5 (2016): 525–527.

30. A. Roberts, H. Pimentel, C. Trapnell, and L. Pachter, "Identification of Novel Transcripts in Annotated Genomes Using RNA-Seq," *Bioinformatics* 27, no. 17 (2011): 2325–2329.

31. C. Soneson, M. I. Love, and M. D. Robinson, "Differential Analyses for RNA-Seq: Transcript-Level Estimates Improve Gene-Level Inferences," *F1000Res* 4 (2015): 1521.

32. S. W. Wingett and S. Andrews, "FastQ Screen: A Tool for Multi-Genome Mapping and Quality Control," *F1000Res* 7 (2018): 1338.

33. L. Kolberg, U. Raudvere, I. Kuzmin, P. Adler, J. Vilo, and H. Peterson, "G:Profiler-Interoperable Web Service for Functional Enrichment Analysis and Gene Identifier Mapping (2023 Update)," *Nucleic Acids Research* 51, no. W1 (2023): W207–W212.

34. J. Reimand, R. Isserlin, V. Voisin, et al., "Pathway Enrichment Analysis and Visualization of Omics Data Using g:Profiler, GSEA, Cytoscape and EnrichmentMap," *Nature Protocols* 14, no. 2 (2019): 482–517.

35. J. Reimand, M. Kull, H. Peterson, J. Hansen, and J. Vilo, "G:Profiler—A Web-Based Toolset for Functional Profiling of Gene Lists From Large-Scale Experiments," *Nucleic Acids Research* 35, no. Web Server issue (2007): W193–W200.

36. M. Kanehisa, M. Furumichi, Y. Sato, M. Kawashima, and M. Ishiguro-Watanabe, "KEGG for Taxonomy-Based Analysis of Pathways and Genomes," *Nucleic Acids Research* 51, no. D1 (2023): D587–D592.

37. E. Cerami, J. Gao, U. Dogrusoz, et al., "The cBio Cancer Genomics Portal: An Open Platform for Exploring Multidimensional Cancer Genomics Data," *Cancer Discovery* 2, no. 5 (2012): 401–404.

38. I. de Bruijn, R. Kundra, B. Mastrogiacomo, et al., "Analysis and Visualization of Longitudinal Genomic and Clinical Data From the AACR Project GENIE Biopharma Collaborative in cBioPortal," *Cancer Research* 83, no. 23 (2023): 3861–3867.

39. J. Gao, B. A. Aksoy, U. Dogrusoz, et al., "Integrative Analysis of Complex Cancer Genomics and Clinical Profiles Using the cBioPortal," *Science Signaling* 6, no. 269 (2013): pl1.

40. M. Plummer, "JAGS: A Program for Analysis of Bayesian Graphical Models Using Gibbs Sampling," in *3rd International Workshop on Distributed Statistical Computing (DSC 2003); Vienna, Austria 124* (R Project, 2003).

41. F. Liu, Y. Gao, B. Xu, et al., "PEG10 Amplification at 7q21.3 Potentiates Large-Cell Transformation in Cutaneous T-Cell Lymphoma," *Blood* 139, no. 4 (2022): 554–571.

42. T. Barrett, S. E. Wilhite, P. Ledoux, et al., "NCBI GEO: Archive for Functional Genomics Data Sets—Update," *Nucleic Acids Research* 41, no. D1 (2012): D991–D995.

43. R. Edgar, M. Domrachev, and A. E. Lash, "Gene Expression Omnibus: NCBI Gene Expression and Hybridization Array Data Repository," *Nucleic Acids Research* 30, no. 1 (2002): 207–210.

44. Z. Wang, N. Liu, S. Shi, S. Liu, and H. Lin, "The Role of PIWIL4, an Argonaute Family Protein, in Breast Cancer," *Journal of Biological Chemistry* 291, no. 20 (2016): 10646–10658.

45. R. P. K. Gill, J. Gantchev, A. Martinez Villarreal, et al., "Understanding Cell Lines, Patient-Derived Xenograft and Genetically Engineered Mouse Models Used to Study Cutaneous T-Cell Lymphoma," *Cells* 11, no. 4 (2022): 593.

46. P. Genzor, S. C. Cordts, N. V. Bokil, and A. D. Haase, "Aberrant Expression of Select piRNA-Pathway Genes Does Not Reactivate piRNA Silencing in Cancer Cells," *Proceedings of the National Academy of Sciences of the United States of America* 116, no. 23 (2019): 11111–11112.

47. E. Olsen, E. Vonderheid, N. Pimpinelli, et al., "Revisions to the Staging and Classification of Mycosis Fungoides and Sezary Syndrome: A Proposal of the International Society for Cutaneous Lymphomas (ISCL) and the Cutaneous Lymphoma Task Force of the European Organization of Research and Treatment of Cancer (EORTC)," *Blood* 110, no. 6 (2007): 1713–1722, https://doi.org/10.1182/blood-2007-03-055749.

48. E. Netchiporouk, J. Gantchev, M. Tsang, et al., "Analysis of CTCL Cell Lines Reveals Important Differences Between Mycosis Fungoides/Sezary Syndrome vs. HTLV-1(+) Leukemic Cell Lines," *Oncotarget* 8, no. 56 (2017): 95981–95998.

49. W. E. Damsky and J. Choi, "Genetics of Cutaneous T Cell Lymphoma: From Bench to Bedside," *Current Treatment Options in Oncology* 17, no. 7 (2016): 33.

50. T. P. Chang and I. Vancurova, "NFkappaB Function and Regulation in Cutaneous T-Cell Lymphoma," *American Journal of Cancer Research* 3, no. 5 (2013): 433–445.

51. E. J. Kim, S. Hess, S. K. Richardson, et al., "Immunopathogenesis and Therapy of Cutaneous T Cell Lymphoma," *Journal of Clinical Investigation* 115, no. 4 (2005): 798–812.

52. S. M. Kaech and W. Cui, "Transcriptional Control of Effector and Memory CD8+ T Cell Differentiation," *Nature Reviews. Immunology* 12, no. 11 (2012): 749–761.

53. M. Kunzli and D. Masopust, "CD4(+) T Cell Memory," *Nature Immunology* 24, no. 6 (2023): 903–914.

54. G. O. Rangel Rivera, H. M. Knochelmann, C. J. Dwyer, et al., "Fundamentals of T Cell Metabolism and Strategies to Enhance Cancer Immunotherapy," *Frontiers in Immunology* 12 (2021): 645242.

55. M. Reina-Campos, N. E. Scharping, and A. W. Goldrath, "CD8(+) T Cell Metabolism in Infection and Cancer," *Nature Reviews. Immunology* 21, no. 11 (2021): 718–738.

56. A. J. Simpson, O. L. Caballero, A. Jungbluth, Y. T. Chen, and L. J. Old, "Cancer/Testis Antigens, Gametogenesis and Cancer," *Nature Reviews Cancer* 5, no. 8 (2005): 615–625.

57. E. Fratta, S. Coral, A. Covre, et al., "The Biology of Cancer Testis Antigens: Putative Function, Regulation and Therapeutic Potential," *Molecular Oncology* 5, no. 2 (2011): 164–182.

58. H. Becker, G. Marcucci, K. Maharry, et al., "Mutations of the Wilms Tumor 1 Gene (WT1) in Older Patients With Primary Cytogenetically Normal Acute Myeloid Leukemia: A Cancer and Leukemia Group B Study," *Blood* 116, no. 5 (2010): 788–792.

59. C. Zhang, G. Bai, W. Zhu, D. Bai, and G. Bi, "Identification of miRNA-mRNA Network Associated With Acute Myeloid Leukemia Survival," *Medical Science Monitor* 23 (2017): 4705–4714.

60. D. Y. Gao, Y. Ling, X. L. Lou, Y. Y. Wang, and L. M. Liu, "GTSF1 Gene May Serve as a Novel Potential Diagnostic Biomarker for Liver Cancer," *Oncology Letters* 15, no. 3 (2018): 3133–3140.

61. P. Horna, L. C. Moscinski, L. Sokol, and H. Shao, "Naive/Memory T-Cell Phenotypes in Leukemic Cutaneous T-Cell Lymphoma: Putative Cell of Origin Overlaps Disease Classification," *Cytometry Part B: Clinical Cytometry* 96, no. 3 (2019): 234–241.

62. J. J. Ipsaro and L. Joshua-Tor, "Developmental Roles and Molecular Mechanisms of Asterix/GTSF1," *Wiley Interdisciplinary Reviews RNA* 13, no. 5 (2022): e1716.

63. M. Tsang, J. Gantchev, E. Netchiporouk, et al., "A Study of Meiomitosis and Novel Pathways of Genomic Instability in Cutaneous T-Cell Lymphomas (CTCL)," *Oncotarget* 9, no. 102 (2018): 37647–37661.

64. E. Lee, N. A. Lokman, M. K. Oehler, C. Ricciardelli, and F. Grutzner, "A Comprehensive Molecular and Clinical Analysis of the piRNA Pathway Genes in Ovarian Cancer," *Cancers (Basel)* 13, no. 1 (2020): 4, https://doi.org/10.3390/cancers13010004.

65. J. J. Campbell, R. A. Clark, R. Watanabe, and T. S. Kupper, "Sezary Syndrome and Mycosis Fungoides Arise From Distinct T-Cell Subsets: A Biologic Rationale for Their Distinct Clinical Behaviors," *Blood* 116, no. 5 (2010): 767–771.

66. J. Strobl and M. Haniffa, "Functional Heterogeneity of Human Skin-Resident Memory T Cells in Health and Disease," *Immunological Reviews* 316 (2023): 104–119.

67. R. Fonseca, L. K. Beura, C. F. Quarnstrom, et al., "Developmental Plasticity Allows Outside-In Immune Responses by Resident Memory T Cells," *Nature Immunology* 21, no. 4 (2020): 412–421.

68. J. Iqbal, D. D. Weisenburger, T. C. Greiner, et al., "Molecular Signatures to Improve Diagnosis in Peripheral T-Cell Lymphoma and Prognostication in Angioimmunoblastic T-Cell Lymphoma," *Blood* 115, no. 5 (2010): 1026–1036, https://doi.org/10.1182/blood-2009-06-227579.

Supporting Information

Additional supporting information can be found online in the Supporting Information section.